Characterisation of frequency-domain loading profiles in high-performance youth badminton players: exploring limb asymmetry across injury history groups

Williams, Jonathan, Luo, Jin ORCID logoORCID: https://orcid.org/0000-0001-5451-9535, Wylde, Matthew and Callaway, Andrew (2026) Characterisation of frequency-domain loading profiles in high-performance youth badminton players: exploring limb asymmetry across injury history groups. Journal of Biomechanics, 206. ISSN 0021-9290

https://doi.org/10.1016/j.jbiomech.2026.113485

Journal of Biomechanics 206 (2026) 113485

Contents lists available at ScienceDirect

Journal of Biomechanics

journal homepage: www.elsevier.com/locate/jbiomech

Characterisation of frequency-domain loading profiles in high-performance youth badminton players: exploring limb asymmetry across injury history groups☆

Jonathan M. Williams [a,*], Jin Luo [b], Matthew J. Wylde [c,1], Andrew J. Callaway [a]

[a] School of Allied Health and Exercise Sciences, Bournemouth University, Poole, UK
[b] School of Medicine and Biosciences, University of West London, UK
[c] National Youth Sports Institute, Singapore

ARTICLE INFO

Keywords:
Accelerometer
IMU
Shock transmissibility
Limb-symmetry index
Attenuation

ABSTRACT

Mechanical loading can be beneficial or consequential, and it is typically measured through accelerometry in the time-domain. This prevents frequency-specific characteristics underpinning musculoskeletal adaptation and injury risk, from being identified. This study aimed to (1) characterise the frequency-domain loading profile (loading rate, band power and transmissibility) of high-performance youth badminton players across four frequency bands, and (2) determine whether limb symmetry within these bands differs between players with and without a history of injury. Accelerometer data from 90 min of simulated matchplay were collected from 30 players (13 female, 17 male) wearing inertial measurement units on the trunk and bilateral shanks. Data were transformed into four bands using the Fast Fourier Transform (FFT; B1: $0 \leq f < 2$ Hz, B2: $2 \leq f < 5$ Hz, B3: $5 \leq f < 10$ Hz, B4: $10 \leq f < 20$ Hz). Loading rate, band power and band RMS were greater at the shanks than the trunk, with the dominant shank demonstrating greater loading and attenuation than the non-dominant shank across all bands. Descriptive patterns suggested that players with bilateral injury history demonstrated the largest asymmetry for loading rate and band power (−11.6 to −28.7%), favouring the dominant limb, while players with unilateral injury history showed a 0.6–10.4% limb symmetry index favouring the non-injured limb and reduced attenuation on the injured limb, most prominently in B4 ($10 \leq f < 20$ Hz). These findings should be interpreted cautiously given the small subgroup sizes and absence of statistical significance and are considered exploratory. Such methods offer novel insights into sport-specific loading demands, injury risk and rehabilitation.

1. Introduction

The human body is continually exposed to mechanical loads during physical activity, and a key function of the neuromuscular system is to regulate these loads within an appropriate range. This range should be sufficient to stimulate beneficial adaptation yet not high enough to contribute to tissue degeneration or injury. For example, bone density improvements in premenopausal women require iliac crest accelerations to exceed a specific threshold (Vainionpää et al., 2006), whereas elevated ground reaction forces, particularly at higher frequencies, are associated with knee pain and thought to be related to osteoarthritis development (Radin et al., 1991).

Body-worn accelerometry is increasingly used in sport to quantify mechanical load exposure, most commonly as player load, the sum of resultant accelerations. Such measures have provided insights into workload monitoring, injury risk and rehabilitation guidance (Costa et al., 2022; Pillitteri et al., 2024). However, simple summation of acceleration amplitude is not sufficient to capture two important characteristics of mechanical loading. First, it does not adequately reflect the dynamic nature of mechanical loading during human locomotion. Loading rate, defined as the time-derivative of acceleration or force, provides a more appropriate measure (Luo et al., 2025). Dynamic loading is particularly effective in promoting bone adaptation (Rubin & Lanyon, 1984), and loading rate has been positively associated with

☆ This article is part of a special issue entitled: 'Biomechanics in AI Age' published in Journal of Biomechanics.

* Corresponding author.
E-mail addresses: JWilliams@bournemouth.ac.uk (J.M. Williams), Jin.Luo@uwl.ac.uk (J. Luo), M.Wylde@latrobe.edu.au (M.J. Wylde), ACallaway@bournemouth.ac.uk (A.J. Callaway).
[1] Present address: Department of Management, Sport and Tourism, La Trobe University, Melbourne, Australia.

https://doi.org/10.1016/j.jbiomech.2026.113485
Accepted 24 July 2026
Available online 28 July 2026

bone mineral density in middle-aged adults (Chahal et al., 2014). Conversely, excessive dynamic loading may induce damage to tissues, and a high loading rate has also been linked to injury risk in runners (Davis et al., 2016). The second limitation is broadband amplitude measures do not distinguish between the different frequencies at which loading occurs. Low-frequency accelerations associated with walking differ from the high-frequency transients produced during impact, and a simple magnitude measure cannot differentiate between them (Vainionpää et al., 2006). This may be particularly important in sport, where the body is exposed to a mixture of activities or movements spanning a wide range of loading frequencies.

Frequency-domain analysis of acceleration signals addresses both limitations, by decomposing the loading signal into meaningful frequency components. While frequency band definitions vary across studies (Hamill et al., 1995; Luo et al., 2025) with no single consensus, four windows with distinct physiological relevance are proposed here based on previous work (Luo et al., 2025). The first window, the locomotion window (B1: $0 \leq f < 2$ Hz), captures the dominant frequencies associated with gait (Antonsson and Mann, 1985). The second window, the active motion window (B2: $2 \leq f < 5$ Hz), corresponds to the voluntary movement component of the locomotion signal, consistent with active-peak frequencies reported during running (Hamill et al., 1995) and the active (sub-impact) acceleration component identified during walking (Luo et al., 2025). The next window, the osteogenic window (B3: $5 \leq f < 10$ Hz), corresponds to frequencies associated with cortical bone mechanotransduction in controlled loading studies (Warden & Turner, 2004). The last window, the impact shock window (B4: $10 \leq f < 20$ Hz), captures the high-frequency transient generated at foot–ground contact corresponding to the impact peak of the ground reaction force (Blackmore et al., 2016; Shorten & Winslow, 1992), and greater loading in this range has been associated with increased running injury risk (Malisoux et al., 2021; Kiernan et al., 2025).

Mechanical loads propagate from the foot–ground interface through the musculoskeletal system, traveling as a shockwave from distal to proximal anatomical regions (Shorten & Winslow, 1992). The efficiency of this transmission (transmissibility) is the ratio of acceleration amplitude between proximal and distal segments (Derrick et al., 1998), and is modulated by both passive structures, including bone, cartilage and connective tissue (Xiang et al., 2022), and active mechanisms such as muscle contraction (Derrick et al., 1998). Critically, attenuation is not uniform across frequencies and the mechanism used to attenuate shock in each frequency band shifts the mechanical burden to the structures associated with that mechanism (Kiernan et al., 2025). Injured runners demonstrated greater 10–20 Hz attenuation between the tibia and sacrum compared to uninjured runners (Kiernan et al., 2025), suggesting that frequency-specific transfer functions may detect injury-related differences in neuromechanical control (Kiernan et al., 2025). To date, neither frequency-domain loading nor transmissibility have been examined in dynamic court sports.

Badminton is characterised by periods of high-intensity multidirectional activity interspersed with short rest periods (Alcock & Cable, 2009), with lower limb injury incidence of 3.4 per 1000 playing hours accounting for up to 54% of all injuries in elite players (Guermont et al., 2021). Structural lower limb asymmetries have also been reported, including greater patellar and Achilles tendon thickness in the dominant leg (Bravo-Sanchez et al., 2019), which are of concern given their association with injury risk (Helme et al., 2021). Using limb-mounted IMUs in adolescent badminton players, Wylde et al. (2022) demonstrated that players with a history of unilateral lower limb injury exhibited loading asymmetries exceeding the 10% clinical threshold, potentially reflecting a protective mechanism or impaired function. Whether such asymmetries extend to specific frequency bands, and whether transmissibility differs between injured and uninjured limbs in this population, remains unknown.

Understanding the frequency-domain loading profile within sport has the potential to provide novel insights into sport-specific loading demands, movement modification in response to injury, and targets for rehabilitation and return-to-play decision making. The aims of this study were to (1) characterise the frequency-domain loading profile of badminton players across four biomechanically defined frequency bands, including loading rate, power spectral density and transmissibility, and (2) determine whether limb symmetry within these frequency bands differs between players with and without a history of lower limb injury. Based on previous work in this population (Wylde et al., 2022) and evidence of altered loading strategies in injured athletes (Kiernan et al., 2025), it was anticipated that players with a history of unilateral injury would demonstrate greater asymmetry favouring the non-injured limb, particularly in higher frequency bands. Given the exploratory nature of Aim 2 and the small subgroup sizes, the study was considered hypothesis-generating for between-group comparisons. Characterisation of the frequency-domain loading profile (Aim 1) provides the empirical basis for interpretation of between-group differences (Aim 2).

2. Methods

2.1. Study design

This study employed a cross-sectional, observational design. Three VXSport inertial measurement units (Visuallex Sport International, Lower Hutt, New Zealand; dimensions: 74 mm × 47 mm × 17 mm; weight: 50 g) were worn by each player. For the trunk sensor, each player wore the manufacturer's elasticised, purpose-built harness with the sensor housed in a dedicated insert, positioned over the upper thoracic spine (T3-T4). Visual inspection was used to confirm a tight fit, minimising movement between sensor and skin (Wylde et al., 2022). For the lower limb sensors, one was placed over each tibia, (located on the anteromedial flare, halfway between the tibial plateau and medial malleolus), reinforced with elastic tape (Wylde et al., 2022). Tri-axial linear acceleration data were collected and stored on the devices at 100 Hz during 90 min of simulated matchplay at a high-performance training centre. Ethical approval was granted by the Singapore Sport Institute Institutional Review Board.

2.2. Participants

Thirty adolescent badminton players (13 female and 17 male) were recruited from a national youth training squad (Age: 14.3 ± 1.2 y, Height: 1.64 ± 0.10 m, Mass: 54.4 ± 9.5 kg, Playing Experience: 7.3 ± 1.7 y). All players were cleared by a certified sports physiotherapist prior to participation. Informed assent was obtained from all participants, and informed consent was obtained from each participant's parent/legal guardian. Players completed a questionnaire reporting lower limb injury in the previous 24 months and for Aim 2 were assigned to one of three groups: no injury history, unilateral injury history (one lower limb), or bilateral injury history (both lower limbs). An injury was defined as a physical complaint preventing normal training for three consecutive sessions. The dominant limb was defined as the self-reported preferred kicking leg (van Melick et al., 2017).

2.3. Data collection

Players completed the team's standardised warm-up before data collection, comprising of jogging, joint mobilising, resistance bands and movement and footwork drills. Simulated matchplay consisted of multiple matches, with players matched by the coach for age, gender and playing ability. Following data collection, units were docked and raw data extracted using VXSport software.

2.4. Data processing

Raw acceleration data was transferred to Matlab 2023b (MathWorks, Natick, MA, USA) for processing. Resultant acceleration was computed as:

$$R = \sqrt{a_x^2 + a_y^2 + a_z^2} \tag{1}$$

Data were bandpass filtered using a 5th order Butterworth filter (0.1–20 Hz), selected following visual inspection of power spectral density (PSD) plots which confirmed negligible signal energy above 20 Hz. The filtered signal was transformed to the frequency-domain using the Fast Fourier Transform (FFT).

Four frequency bands were defined with their boundaries informed by a combination of prior literature and empirical observation of acceleration spectra. This revealed a primary spectral peak at ~ 1 to 2 Hz, a secondary peak at ~ 3 to 4 Hz with a trough at ~ 2 Hz, rapid spectral decay above 5 Hz, and no meaningful signal above 15 Hz. Bands were therefore defined as: B1 ($0 \leq f < 2$ Hz), B2 ($2 \leq f < 5$ Hz), B3 ($5 \leq f < 10$ Hz), and B4 ($10 \leq f < 20$ Hz) with physiological rationale and labelling for each band described in the Introduction.

The following outcome measures were calculated for the right shank, left shank and trunk at each frequency band.

Frequency-domain loading rate, defined as the rate of change of acceleration within a frequency band and was calculated based on the work of Luo et al., (2025):

$$LR_{band} = \sum_{n=i}^{j} A_n \times f_n \tag{2}$$

where LR_{band}(g/s) is the loading rate from the i^{th} to j^{th} harmonic, A_n(g) is the acceleration amplitude at the n^{th} harmonic from a single FFT of the full filtered signal, and f_n(Hz) is the corresponding harmonic frequency. The frequency resolution of the FFT was $\Delta f = f_s/N$, where $f_s = 100$ Hz and N is the total number of samples in the trial. As loading rate was derived from accelerometry rather than force plate data, values are expressed in g/s rather than the conventional N/s or BW/s used in force-based studies. Luo et al. (2025) demonstrated that frequency-domain loading rate correlates significantly with time-domain measures including average loading rate and instantaneous loading rate derived from ground reaction forces.

Band power, defined as the magnitude of acceleration energy within a frequency band, was calculated using equation (3):

$$P_{band} = \sum_{f=f_i}^{f_j} PSD(f) \cdot \Delta f \tag{3}$$

where P_{band}(g^2) is the power from f_i to f_j, PSD(f)(g^2/Hz) is the power spectral density at frequency f estimated using Welch's method, and Δf (Hz) is the frequency resolution. PSD was estimated using Welch's method (Hann window, 512 samples, 50% overlap, FFT length 512 points; frequency resolution ~0.195 Hz.

Band RMS, defined as the root mean square acceleration within a frequency band, was calculated using equation (4):

$$RMS_{band} = \sqrt{P_{band}} \tag{4}$$

where RMS_{band}(g) represents the effective acceleration magnitude within the band.

Percentage power, defined as the relative distribution of acceleration energy across frequency bands, was calculated using equation (5):

$$\%P_{band} = \frac{P_{band}}{\sum_{k=1}^{K} P_k} \times 100 \tag{5}$$

where $\%P_{band}$(%) is the proportion of total power in the band of interest, independent of the player work duration. $\sum_{k=1}^{K} Pk$ is the sum of power across all K frequency bands.

Transmissibility, defined as the amplitude ratio between trunk to shank PSD at each frequency, was calculated as:

$$T(f) = \sqrt{\frac{PSD_{trunk}(f)}{PSD_{shin}(f)}} \tag{6}$$

where T(f) represents a dimensionless amplitude transmissibility at frequency f, $PSD_{Trunk}(f)$ (g ^{2}/H z) is the power spectral density at the trunk and $PSD_{shin}(f)$(g^2/Hz) is the power spectral density at the shank. The square root is applied to convert from a power ratio to an amplitude ratio. Band-averaged transmissibility was calculated as a PSD weighted average:

$$T_{band} = \frac{\sum_{f=f_i}^{f_j} T(f) \cdot PSD_{shin}(f) \cdot \Delta f}{\sum_{f=f_i}^{f_j} PSD_{shin}(f) \cdot \Delta f} \tag{7}$$

where weighting by $PSD_{shin}(f)$ ensures frequencies with greater input energy at the shank contribute proportionally more to the band average. Band transmissibility was expressed in decibels:

$$T_{band,dB} = 20 \cdot \log_{10}(T_{band}) \tag{8}$$

where the factor of 20 rather than 10 is used because T_{band} is an amplitude rather than power ratio. Negative values indicate attenuation from shank to trunk; positive indicates amplification. This variable defines how efficiently acceleration energy travels from the shank to the trunk. Values close to zero indicate loading is unattenuated.

Limb symmetry index (LSI) was calculated for loading rate, band power and transmissibility using:

$$LSI = \left(1 - \frac{X_{ref}}{X_{comp}}\right) \times 100 \tag{9}$$

where X_{ref} is the reference limb value (dominant for non-injured and bilateral injury history groups; injured limb for unilateral group), and X_{comp} is the comparison limb. Positive values indicate lower loading on the reference limb. An absolute LSI exceeding 10% was considered clinically meaningful, consistent with established return-to-sport criteria (Schmitt et al., 2012; Wylde et al., 2022).

For transmissibility LSI, a difference rather than ratio was computed using:

$$LSI_T = T_{band,dB(ref)} - T_{band,dB(comp)} \tag{10}$$

as subtraction of log-scale values is equivalent to the logarithm of their ratio. A negative value indicates that the reference limb attenuates impact energy more efficiently than the comparison limb; a positive value indicates the comparison limb attenuates more efficiently. In the context of injury, a positive transmissibility LSI in the unilateral group would suggest the non-injured limb (comparison limb) is absorbing greater impact energy.

2.5. Statistics

Due to the limited sample size and subsequent sub-grouping for Aim 2, non-parametric statistics were used throughout. All statistical testing was completed in Matlab 2023b (MathWorks, Natick, MA, USA). Differences in loading profiles across anatomical locations (dominant shank, non-dominant shank and trunk) were explored using the Friedman test with Wilcoxon signed-rank post-hoc comparisons. Between-group differences in LSI were explored using Kruskal-Wallis testing. Bonferroni correction was applied for all multiple comparisons.

LSI was computed for loading rate, band power, and transmissibility. Band RMS was excluded as it is mathematically equivalent to band power (RMS = $\sqrt{\text{Power}}$) and would yield identical rank-order comparisons. Percentage power was similarly excluded as Aim 1 demonstrated symmetric spectral distribution between limbs.

Effect size was reported as eta-squared (η^2) for Kruskal-Wallis tests (small ≥ 0.01, medium ≥ 0.06, large ≥ 0.14; Cohen, 1988) and as r = Z/

$\sqrt{N}$ for Wilcoxon signed-rank tests (small ≥ 0.10, medium ≥ 0.30, large ≥ 0.50; Cohen, 1988).

3. Results

3.1. Whole group analysis

Median and interquartile range for frequency-domain loading profiles across 2700 min of badminton matchplay are presented in Tables 1a–e.

Loading rate, band power and band RMS were significantly greater at both shanks than the trunk across all frequency bands (Tables 1a–c, Fig. 1 for Loading rate), with the dominant shank demonstrating significantly greater absolute loading than the non-dominant shank across all bands.

Expressed as a percentage of total power, significant shank-trunk differences were observed at B2, B3 and B4, but no between-shank differences were found at any band (Table 1d, Fig. 1). Percentage power did not differ across anatomical locations at B1 ($p = 0.061$). Approximately 70% of shank power was distributed across B1 and B2 in roughly equal proportions (~35% each), reflecting locomotion and change of direction demands. At the trunk, B2 was the dominant band (~42%), representing a proportionally greater contribution from step-frequency harmonics and active lower-limb movement coordination compared to the shank.

Transmissibility ranged from approximately −4 to −8 dB across bands, indicating consistent attenuation from shank to trunk. The dominant shank demonstrated significantly greater attenuation than the non-dominant shank across all frequency bands (Table 1e, Fig. 1). Transmissibility was calculated independently for each limb as the ratio of trunk to shank PSD; whilst dominant shank input loading was greater than non-dominant across all bands (Table 1a), between-limb transmissibility differences therefore reflect relative attenuation efficiency rather than absolute loading magnitude.

3.2. Injury history sub-group analysis

Median LSI for loading rate, band power and transmissibility by injury group are presented in Tables 2a-2c, Fig. 2. No significant between-group differences were identified following Kruskal-Wallis testing with Bonferroni correction (all $p > 0.05$), which may reflect limited statistical power given the small group sizes (UI $n = 7$, BI $n = 5$). However, effect sizes ranged from small to moderate (η^2 = 0.063–0.217), with the largest effect size consistently observed within the B4 band.

Descriptively, a consistent pattern was observed across all LSI variables and frequency bands. The bilateral group demonstrated the most negative LSI values (loading rate: −11.57 to −15.70%; power: –22.14 to −28.68%), suggesting higher loading on the dominant limb. The non-injured group showed intermediate negative values (loading rate: −2.22 to −8.27%; power: −5.18 to −11.54%), suggesting dominant limb preferential loading as observed in the whole group analysis. The unilateral group demonstrated LSI values close to or just above zero (loading rate: 0.62 to 5.56%; power: 0.89 to 10.41%), suggesting a shift in loading away from the injured limb, with greater within-group variability than the other groups (IQR spanning up to 29 percentage points for loading rate at B1).

For transmissibility LSI, the bilateral group showed the most negative values (−0.75 to −1.09 dB), suggesting greater dominant-side attenuation. The unilateral group showed positive values (0.04 to 0.48 dB), suggesting reduced attenuation on the injured limb.

4. Discussion

The purpose of this study was to characterise, for the first time, the frequency-domain loading profile of youth high-performance badminton players. This was successfully achieved, demonstrating distinct loading profiles for the shank and trunk. Loading rate was significantly greater at the shanks compared to the trunk across all frequency bands. The largest absolute difference between shank and trunk was observed in the B4 band, demonstrating the ability of the trunk to selectively filter high-frequency impact energy. All pairwise comparisons between anatomical locations demonstrated large effect sizes (r = 0.51 – 0.79). Moreover, the proportional shift towards the B2 band at the trunk demonstrates the relative dominance of active movement-related frequencies at this location, potentially reflecting the change of direction demands of badminton. Critically, this finding extends previous frequency-domain work (Luo et al., 2025) beyond straight-line walking to the complex, multidirectional movement demands characteristic of court-based sport.

The current study identified significant differences in transmissibility, with the dominant limb demonstrating greater attenuation compared to the non-dominant limb, across all frequency bands (Table 1e; $r = 0.55$–0.63, large effect). Previous studies examining shock attenuation have either focused on a single limb (Hamill et al., 1995; Kiernan et al., 2025), or found no between limb differences (Desai et al.,

Table 1a
Frequency-domain loading rate (g/s) across four frequency bands ($n = 30$).

Band	Dominant Shank	Non-Dominant Shank	Trunk	Location Effect	Effect size
	Median (IQR)	*Median (IQR)*	*Median (IQR)*	*Friedman/Pairwise*[a]	r
B1 (0–2 Hz)	49.13 (42.78–55.22)	42.07 (38.94–51.32)	29.29 (27.44–32.28)	Friedman: $p < 0.001$ D vs ND: $p < 0.001$ D vs T: $p < 0.001$ ND vs T: $p < 0.001$	0.787
B2 (2–5 Hz)	200.54 (188.14–235.28)	193.33 (172.14–218.44)	115.34 (96.02–125.73)	Friedman: $p < 0.001$ D vs ND: $p = 0.015$ D vs T: $p < 0.001$ ND vs T: $p < 0.001$	0.513
B3 (5–10 Hz)	435.43 (373.42–481.20)	387.32 (351.22–433.17)	170.28 (147.80–214.00)	Friedman: $p < 0.001$ D vs ND: $p = 0.001$ D vs T: $p < 0.001$ ND vs T: $p < 0.001$	0.637
B4 (10–20 Hz)	1020.53 (878.24–1095.61)	909.45 (812.11–995.63)	374.65 (293.65–463.35)	Friedman: $p < 0.001$ D vs ND: $p = 0.006$ D vs T: $p < 0.001$ ND vs T: $p < 0.001$	0.565

D = Dominant Shank; ND = Non-Dominant Shank; T = Trunk.
[a] Friedman test (repeated measures) across three anatomical locations. Pairwise Wilcoxon signed-rank follow-up with Bonferroni correction (×3; corrected $\alpha = 0.017$). Effect size $r = Z/\sqrt{N}$; small ≥ 0.10, medium ≥ 0.30, large ≥ 0.50 (Cohen, 1988).

Table 1b
Band power (g^2) across four frequency bands (n = 30).

Band	Dominant Shank *Median (IQR)*	Non-Dominant Shank *Median (IQR)*	Trunk *Median (IQR)*	Location Effect *Friedman/Pairwise*[a]	Effect size *r*
B1 (0–2 Hz)	0.149 (0.123–0.199)	0.126 (0.106–0.175)	0.043 (0.037–0.056)	Friedman: $p < 0.001$ D vs ND: $p = 0.001$ D vs T: $p < 0.001$ ND vs T: $p < 0.001$	0.652
B2 (2–5 Hz)	0.150 (0.125–0.189)	0.133 (0.108–0.168)	0.053 (0.037–0.064)	Friedman: $p < 0.001$ D vs ND: $p = 0.012$ D vs T: $p < 0.001$ ND vs T: $p < 0.001$	0.528
B3 (5–10 Hz)	0.083 (0.065–0.108)	0.072 (0.056–0.086)	0.014 (0.011–0.021)	Friedman: $p < 0.001$ D vs ND: $p = 0.011$ D vs T: $p < 0.001$ ND vs T: $p < 0.001$	0.531
B4 (10–20 Hz)	0.061 (0.046–0.071)	0.050 (0.039–0.059)	0.009 (0.006–0.014)	Friedman: $p < 0.001$ D vs ND: $p = 0.010$ D vs T: $p < 0.001$ ND vs T: $p < 0.001$	0.535

D = Dominant Shank; ND = Non-Dominant Shank; T = Trunk.
[a] Friedman test (repeated measures) across three anatomical locations. Pairwise Wilcoxon signed-rank follow-up with Bonferroni correction (×3; corrected $\alpha = 0.017$). Effect size $r = Z/\sqrt{N}$; small ≥ 0.10, medium ≥ 0.30, large ≥ 0.50 (Cohen, 1988).

Table 1c
Band RMS (g) across four frequency bands (n = 30).

Band	Dominant Shank *Median (IQR)*	Non-Dominant Shank *Median (IQR)*	Trunk *Median (IQR)*	Location Effect *Friedman/Pairwise*[a]	Effect size *r*
B1 (0–2 Hz)	0.386 (0.351–0.446)	0.355 (0.326–0.418)	0.207 (0.192–0.237)	Friedman: $p < 0.001$ D vs ND: $p < 0.001$ D vs T: $p < 0.001$ ND vs T: $p < 0.001$	0.670
B2 (2–5 Hz)	0.387 (0.354–0.435)	0.365 (0.329–0.410)	0.230 (0.192–0.253)	Friedman: $p < 0.001$ D vs ND: $p = 0.007$ D vs T: $p < 0.001$ ND vs T: $p < 0.001$	0.554
B3 (5–10 Hz)	0.288 (0.255–0.329)	0.268 (0.237–0.293)	0.118 (0.105–0.145)	Friedman: $p < 0.001$ D vs ND: $p = 0.004$ D vs T: $p < 0.001$ ND vs T: $p < 0.001$	0.584
B4 (10–20 Hz)	0.247 (0.214–0.266)	0.224 (0.197–0.243)	0.095 (0.077–0.118)	Friedman: $p < 0.001$ D vs ND: $p = 0.006$ D vs T: $p < 0.001$ ND vs T: $p < 0.001$	0.565

D = Dominant Shank; ND = Non-Dominant Shank; T = Trunk.
[a] Friedman test (repeated measures) across three anatomical locations. Pairwise Wilcoxon signed-rank follow-up with Bonferroni correction (×3; corrected $\alpha = 0.017$). Effect size $r = Z/\sqrt{N}$; small ≥ 0.10, medium ≥ 0.30, large ≥ 0.50 (Cohen, 1988).

2024). The findings by Desai et al. (2024) in recreational runners, contrasts with the current study, suggesting that dominant limb attenuation superiority is not a general phenomenon but rather a sport-specific adaptation associated with the demands of badminton. Whether this reflects structural asymmetry in lower limb muscle architecture driven by racquet sports (Bravo-Sanchez et al., 2019), asymmetric neuromuscular control strategies, or the multidirectional loading demands of the sport remains unclear and warrants further investigation. Interestingly, the largest effect sizes were observed in the B3 and B4 bands, suggesting that high-frequency impact shock, likely most associated with court landings and jump smash actions, may be particularly important in driving the asymmetry. This finding is consistent with the high-impact, asymmetric nature of badminton-specific movement demonstrated previously (Wylde et al., 2022).

The results suggest a pattern of loading across the three sub-groups, though the small subgroup sizes and absence of statistical significance require that these observations are interpreted with caution. Frequency-domain LSI suggest directional and band-specific patterns of asymmetry, extending the previous literature beyond broadband vector magnitude (Wylde et al., 2022). The players with no previous injury showed a pattern towards asymmetry favouring the dominant limb for LR and power, but this remains below the 10% clinical significance window (Schmitt et al., 2012). The players with a history of unilateral injury showed a pattern towards a switch to favour the non-injured limb across all bands, while the players with bilateral injury history showed asymmetry up to 16%, favouring the dominant limb. The results suggest this asymmetry pattern is most pronounced within the B4 band, implying that high-frequency impact shocks may exert a substantial influence on the observed asymmetry across the three sub-groups.

To date, no studies have explored the LSI for transmissibility in a sport-specific context. Kiernan et al. (2025) compared transmissibility between previously injured and non-injured runners, finding greater lower-body attenuation in those with injury history. In contrast, the current study observed reduced attenuation on the injured limb in the unilateral injury group, consistent with the loading rate and band power LSI findings, where the injured limb showed lower overall loading. The non-injured and bilateral injury history groups demonstrated small and more pronounced negative transmissibility LSI values respectively (range: −0.20 to −0.48 dB and −0.75 to −1.09 dB), consistent with the dominant limb attenuation superiority observed in Aim 1 and mirroring the loading rate and band power findings in the bilateral group. Whether this reflects a neuromuscular response to mitigate impact loading or an

Table 1d
Percentage power distribution across frequency bands (n = 30).

Band	Dominant Shank	Non-Dominant Shank	Trunk	Location Effect	Effect size
	Median (IQR)	*Median (IQR)*	*Median (IQR)*	*Friedman/ Pairwise*[a]	*r*
B1 (0–2 Hz)	35.7 (34.2–37.1)	34.8 (33.2–37.8)	37.1 (34.6–41.7)	Friedman: $p = 0.063$	0.351
B2 (2–5 Hz)	34.6 (33.2–35.5)	34.5 (33.1–35.8)	41.9 (39.5–43.9)	Friedman: $p < 0.001$ D vs ND: $p = 0.955$ D vs T: $p < 0.001$ ND vs T: $p < 0.001$	−0.182
B3 (5–10 Hz)	18.2 (17.2–18.9)	18.0 (17.5–18.8)	12.7 (10.6–14.5)	Friedman: $p < 0.001$ D vs ND: $p = 0.868$ D vs T: $p < 0.001$ ND vs T: $p < 0.001$	−0.193
B4 (10–20 Hz)	12.6 (11.4–13.4)	12.5 (11.2–13.1)	7.4 (6.2–9.2)	Friedman: $p < 0.001$ D vs ND: $p = 0.687$ D vs T: $p < 0.001$ ND vs T: $p < 0.001$	−0.220

D = Dominant Shank; ND = Non-Dominant Shank; T = Trunk.
[a] Friedman test (repeated measures) across three anatomical locations. Pairwise Wilcoxon signed-rank follow-up with Bonferroni correction (×3; corrected $\alpha = 0.017$). Effect size $r = Z/\sqrt{N}$; small ≥ 0.10, medium ≥ 0.30, large ≥ 0.50 (Cohen, 1988). Negative r indicates trunk percentage power exceeds dominant shank.

Table 1e
Transmissibility (dB) from shank to trunk across four frequency bands (n = 30) *Negative values indicate attenuation of the acceleration signal from shin to trunk.*

Band	Dominant Shank to Trunk *Median (IQR)*	Non-Dominant Shank to Trunk *Median (IQR)*	Dom vs Non-Dom[b] *Wilcoxon (Bonf × 4)*	Effect Size *r*
	dB	*dB*		
B1 (0–2 Hz)	−5.72 (−6.59 – −5.24)	−5.12 (−5.89 – −4.62)	*$p = 0.006$*	*0.58*
B2 (2–5 Hz)	−4.75 (−5.87 – −4.24)	−4.32 (−5.11 – −3.42)	*$p = 0.010$*	*0.55*
B3 (5–10 Hz)	−7.43 (−8.10 – −6.40)	−6.91 (−7.44 – −6.18)	*$p = 0.002$*	*0.63*
B4 (10–20 Hz)	−7.80 (−9.09 – −6.64)	−7.58 (−8.41 – −6.60)	*$p = 0.005$*	*0.59*

Dom = Dominant Shank; Non-Dom = Non-Dominant Shank; T = Trunk.
[b] Pairwise Wilcoxon signed-rank (Dominant vs Non-Dominant shank) with Bonferroni correction across 4 bands (×4; corrected $\alpha = 0.013$). Effect size $r = Z/\sqrt{N}$; small ≥ 0.10, medium ≥ 0.30, large ≥ 0.50 (Cohen, 1988).

impairment of function remains unclear and warrants further investigation.

The proposed method demonstrated in this study has the potential to change the understanding of real-world loading exposure offering new insights into injury risk and rehabilitation. Integrating the frequency domain characteristics into existing player monitoring could result in new understandings around the exposure and risk especially chronic overuse type injuries. Moreover, the methods could offer insights into

Table 2a
LSI Loading Rate (%) by injury group across four frequency bands.

Band	Non-Injured (n = 18)	Unilateral (n = 7)	Bilateral (n = 5)	Group Effect[a]	Effect size
	Median (IQR) (%)	*Median (IQR) (%)*	*Median (IQR) (%)*	*KW/ Pairwise*[b]	η^2
B1 (0–2 Hz)	−8.27 (−16.89 to −2.16)	0.80 (−15.03 to 13.98)	−15.70 (−23.23 to −12.48)	KW: $p = 0.431$, NI vs UI: $p = 0.414$ NI vs BI: $p = 0.438$ UI vs BI: $p = 0.447$	0.091
B2 (2–5 Hz)	−2.22 (−8.86 to 0.58)	4.53 (−4.14 to 5.56)	−13.22 (−14.84 to −5.50)	KW: $p = 0.146$, NI vs UI: $p = 0.195$ NI vs BI: $p = 0.328$ UI vs BI: $p = 0.144$	0.171
B3 (5–10 Hz)	−6.04 (−10.26 to 1.00)	0.62 (−5.45 to 2.76)	−11.57 (−13.96 to −8.18)	KW: $p = 0.419$, NI vs UI: $p = 0.954$ NI vs BI: $p = 0.380$ UI vs BI: $p = 0.144$	0.093
B4 (10–20 Hz)	−4.34 (−11.40 to 0.33)	5.56 (−4.03 to 8.39)	−12.73 (−17.57 to −7.66)	KW: $p = 0.079$, NI vs UI: $p = 0.148$ NI vs BI: $p = 0.281$ UI vs BI: $p = 0.053$	0.217

NI = Non-Injured (n = 18); UI = Unilateral Injury (n = 7); BI = Bilateral Injury (n = 5).
LSI = Limb Symmetry Index. For NI and BI groups: LSI = (1 − dominant/non-dominant) × 100. For UI group: LSI = (1 − injured/non-injured) × 100. Positive values indicate lower loading on the reference limb (dominant or injured) relative to the comparison limb. Negative values indicate higher loading on the reference limb relative to the comparison limb.
[a] Kruskal-Wallis test across three groups. Bonferroni correction applied across 4 bands (corrected $\alpha = 0.013$). η^2 = eta-squared effect size.
[b] Pairwise Mann-Whitney U with Bonferroni correction across 3 pairs (corrected $\alpha = 0.017$). Reported regardless of KW significance for transparency.

lingering deficits from a rehabilitation perspective. Underexposure to particular loading frequencies during the rehabilitation process may fail to prepare the player for the rigours of the activity. Future research should seek to understand frequency domain loading profiles for other sports and explore rehabilitation strategies that preferentially result in exposure to specific loading frequencies.

5. Limitations

This study is limited by its cross-sectional design; a longitudinal approach would better characterise the temporal relationship between loading and injury. The study was underpowered for between-group comparisons, based on the largest observed effect size ($\eta^2 = 0.217$, B4 loading rate; $\alpha = 0.05$; $1 - \beta = 0.80$; $k = 3$), 15 participants per group would be required for adequate power. Restricting injury classification may yield more specific findings, particularly given the large interquartile ranges. Sex was not examined as a covariate in the current analyses; future work should consider whether frequency-domain loading and transmissibility profiles differ between male and female players. Data were collected during simulated rather than competitive matchplay.

Table 2b
LSI Band Power (%) by injury group across four frequency bands.

Band	Non-Injured (n = 18) Median (IQR) (%)	Unilateral (n = 7) Median (IQR) (%)	Bilateral (n = 5) Median (IQR) (%)	Group Effect[a] KW/ Pairwise[b]	Effect size η^2
B1 (0–2 Hz)	−7.61 (−23.53 to −3.88)	4.67 (−25.54 to 25.12)	−24.13 (−41.56 to −16.49)	KW: p = 0.218, NI vs UI: p = 0.254 NI vs BI: p = 0.203 UI vs BI: p = 0.447	0.141
B2 (2–5 Hz)	−5.18 (−20.75 to 1.73)	6.83 (−16.38 to 11.94)	−28.68 (−34.49 to −14.11)	KW: p = 0.203, NI vs UI: p = 0.223 NI vs BI: p = 0.380 UI vs BI: p = 0.220	0.147
B3 (5–10 Hz)	−11.54 (−20.81 to 4.01)	0.89 (−20.90 to 7.45)	–22.14 (−28.97 to −16.47)	KW: p = 0.628, NI vs UI: p = 1.000 NI vs BI: p = 0.328 UI vs BI: p = 0.447	0.063
B4 (10–20 Hz)	−7.48 (−22.04 to 1.71)	10.41 (−12.60 to 16.43)	–23.89 (−36.25 to −15.84)	KW: p = 0.113, NI vs UI: p = 0.170 NI vs BI: p = 0.328 UI vs BI: p = 0.091	0.190

NI = Non-Injured (n = 18); UI = Unilateral Injury (n = 7); BI = Bilateral Injury (n = 5).
LSI = Limb Symmetry Index. For NI and BI groups: LSI = (1 − dominant/non-dominant) × 100. For UI group: LSI = (1 − injured/non-injured) × 100. Positive values indicate lower loading on the reference limb (dominant or injured) relative to the comparison limb. Negative values indicate higher loading on the reference limb relative to the comparison limb.
[a] Kruskal-Wallis test across three groups. Bonferroni correction applied across 4 bands (corrected α = 0.013). η^2 = eta-squared effect size.
[b] Pairwise Mann-Whitney U with Bonferroni correction across 3 pairs (corrected α = 0.017). Reported regardless of KW significance for transparency.

6. Conclusion

Frequency-domain analysis revealed distinct mechanical loading profiles during badminton matchplay, with loading rate, band power and band RMS significantly greater at both shanks than the trunk across all frequency bands, and the dominant shank demonstrating greater absolute loading and attenuation. Frequency-domain LSI revealed different directional and band-specific asymmetry where players without injury history showed a pattern towards slightly greater dominant limb loading; those with unilateral injury history showed the opposite, with loading shifting to the non-injured limb, most prominently in the B4 band; and those with bilateral injury history demonstrating the largest asymmetries, favouring the dominant limb. Frequency-domain accelerometry provides a sensitive tool for characterising loading exposure and detecting injury-related asymmetries, with potential applications in workload monitoring, injury risk stratification and rehabilitation.

Table 2c
LSI Transmissibility (dB) by injury group across four frequency bands.

Band	Non-Injured (n = 18) *Median (IQR) (dB)*	Unilateral (n = 7) *Median (IQR) (dB)*	Bilateral (n = 5) *Median (IQR) (dB)*	Group Effect[a] *KW/ Pairwise*[b]	Effect Size η^2
B1 (0–2 Hz)	−0.26 (−0.68 to −0.09)	0.26 (−0.66 to 1.23)	−0.75 (−1.38 to −0.51)	KW: p = 0.196, NI vs UI: p = 0.326 NI vs BI: p = 0.172 UI vs BI: p = 0.318	0.149
B2 (2–5 Hz)	−0.20 (−0.77 to 0.07)	0.38 (−0.63 to 0.52)	−1.09 (−1.27 to −0.55)	KW: p = 0.203, NI vs UI: p = 0.223 NI vs BI: p = 0.380 UI vs BI: p = 0.220	0.147
B3 (5–10 Hz)	−0.48 (−0.84 to 0.19)	0.04 (−0.79 to 0.34)	−0.87 (−1.11 to −0.67)	KW: p = 0.552, NI vs UI: p = 1.000 NI vs BI: p = 0.328 UI vs BI: p = 0.318	0.073
B4 (10–20 Hz)	−0.32 (−0.88 to 0.08)	0.48 (−0.53 to 0.79)	−0.96 (−1.35 to −0.63)	KW: p = 0.094, NI vs UI: p = 0.170 NI vs BI: p = 0.328 UI vs BI: p = 0.053	0.204

NI = Non-Injured (n = 18); UI = Unilateral Injury (n = 7); BI = Bilateral Injury (n = 5).
LSI Transmissibility expressed as the difference in dB between dominant/injured and non-dominant/non-injured shin-to-trunk transmissibility. Negative values indicate greater attenuation on the dominant or injured side.
[a] Kruskal-Wallis test across three groups. Bonferroni correction applied across 4 bands (corrected α = 0.013). η^2 = eta-squared effect size.
[b] Pairwise Mann-Whitney U with Bonferroni correction across 3 pairs (corrected α = 0.017). Reported regardless of KW significance for transparency.

7. Declaration of generative AI and AI-assisted technologies in the manuscript preparation process

During the preparation of this work the author(s) used ClaudeAI in order to check the manuscript for errors. After using this tool/service, the author(s) reviewed and edited the content as needed and take(s) full responsibility for the content of the published article.

CRediT authorship contribution statement

Jonathan M. Williams: Writing – review & editing, Writing – original draft, Methodology, Formal analysis, Conceptualization. **Jin Luo:** Writing – review & editing, Writing – original draft, Methodology, Formal analysis, Conceptualization. **Matthew J. Wylde:** Writing – review & editing, Writing – original draft, Data curation. **Andrew J. Callaway:** Writing – review & editing, Writing – original draft, Methodology, Conceptualization.

Declaration of competing interest

The authors declare that they have no known competing financial interests or personal relationships that could have appeared to influence

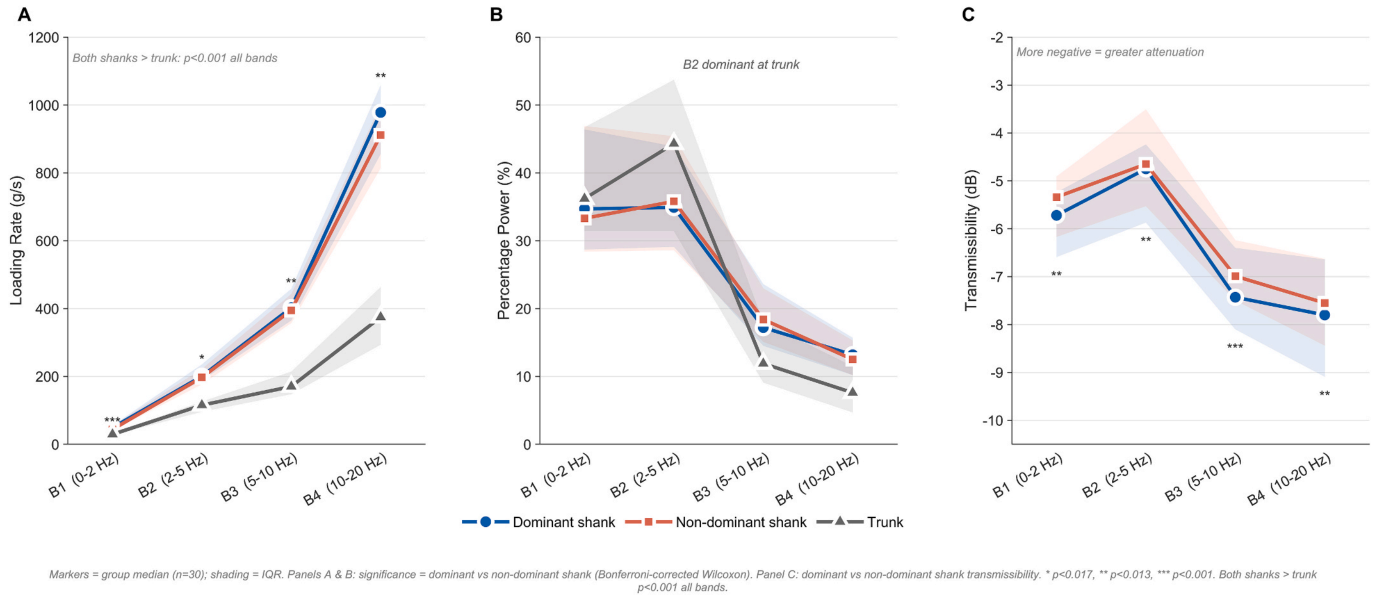

Fig. 1. Whole group Loading Rate, Power Spectral Density (as a percentage of total power) and Transmissibility from shank to trunk. Markers = group median (n = 30); shading = IQR. Panels A & B: significance = dominant vs non-dominant shank (Bonferroni-corrected Wilcoxon). Panel C: dominant vs non-dominant transmissibility. Significance reflects Bonferroni-corrected values* p < 0.017, ** p < 0.013, *** p < 0.001. Both shanks > trunk p < 0.001 all bands.

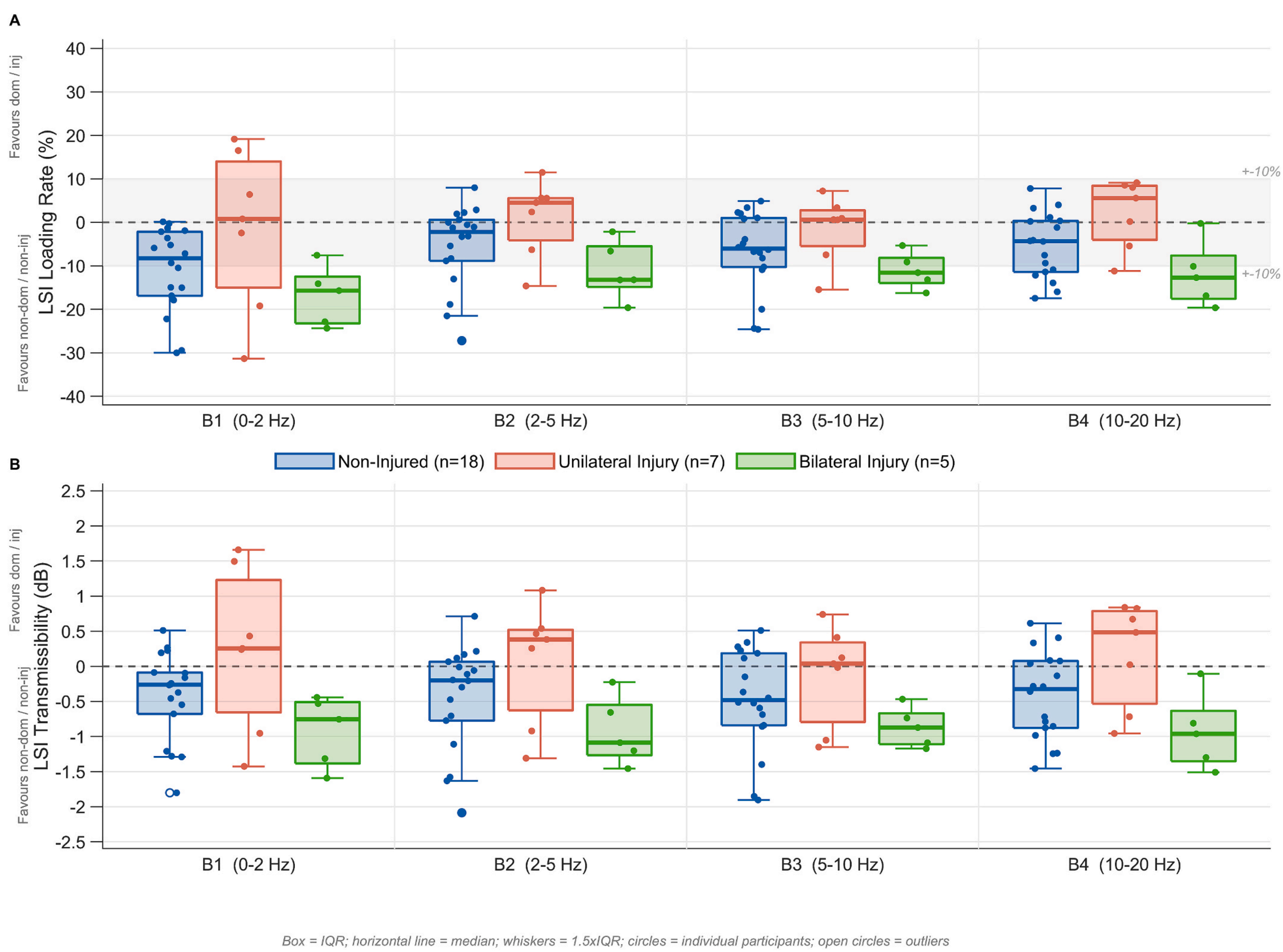

Fig. 2. Box plot of limb symmetry (Loading Rate and Transmissibility LSI) for sub-groups with and without injury history. Shading represents +/- 10%. Box = IQR; horizontal line = median; whiskers = 1.5xIQR; circles = individual participants; open circles = outliers.

the work reported in this paper.

References

Alcock, A., Cable, N.T., 2009. A comparison of singles and doubles Badminton: heart-rate response, player profiles and game characteristics. Int. J. Perform. Anal. Sport 9 (2), 228–237. https://doi.org/10.1080/24748668.2009.11868479.

Antonsson, E., Mann, R., 1985. The frequency content of gait. J. Biomech. 18 (1), 39–47. https://doi.org/10.1016/0021-9290(85)90043-0.

Blackmore, T., Willy, R.W., Creaby, M.W., 2016. The high frequency component of the vertical ground reaction force is a valid surrogate measure of the impact peak. J. Biomech. 49 (3), 479–483. https://doi.org/10.1016/j.jbiomech.2015.12.019.

Bravo-Sanchez, A., Abian, P., Jimenez, F., Abian-Vicen, J., 2019. Myotendinous asymmetries derived from the prolonged practice of badminton in professional players. PLoS One 14 (9), e0222190. https://doi.org/10.1371/journal.pone.0222190.

Chahal, J., Lee, R., Luo, J., 2014. Loading dose of physical activity is related to muscle strength and bone density in middle-aged women. Bone 67, 41–45. https://doi.org/10.1016/j.bone.2014.06.029.

Cohen, J., 1988. *Statistical power analysis for the behavioral sciences*, second ed. Lawrence Erlbaum Associates.

Costa, J.A., Rago, V., Brito, P., Figueiredo, P., Sousa, A., Abade, E., Brito, J., 2022. Training in women soccer players: a systematic review on training load monitoring. Front. Psychol. 13, 943857. https://doi.org/10.3389/fpsyg.2022.943857.

Davis, I.S., Bowser, B.J., Mullineaux, D.R., 2016. Greater vertical impact loading in female runners with medically diagnosed injuries: a prospective investigation. Br. J. Sports Med. 50 (14), 887–892. https://doi.org/10.1136/bjsports-2015-094579.

Derrick, T.R., Hamill, J., Caldwell, G.E., 1998. Energy absorption of impacts during running at various stride lengths. Med. Sci. Sports Exerc. 30 (1), 128–135. https://doi.org/10.1097/00005768-199801000-00018.

Desai, G.A., DeJong Lempke, A.F., Harezlak, J., Gruber, A.H., 2024. Sex differences in body composition and shock attenuation during running. J. Biomech. 173, 112245. https://doi.org/10.1016/j.jbiomech.2024.112245.

Guermont, H., Le Van, P., Marcelli, C., Reboursière, E., Drigny, J., 2021. Epidemiology of injuries in elite Badminton players: a prospective study. Clin. J. Sport Med. 31 (6), 473–475. https://doi.org/10.1097/JSM.0000000000000848.

Hamill, J., Derrick, T.R., Holt, K.G., 1995. Shock attenuation and stride frequency during running. Hum. Mov. Sci. 14 (1), 45–60. https://doi.org/10.1016/0167-9457(95)00004-C.

Helme, M., Tee, J., Emmonds, S., Low, C., 2021. Does lower-limb asymmetry increase injury risk in sport? a systematic review. Phys. Ther. Sport 49, 204–213. https://doi.org/10.1016/j.ptsp.2021.03.001.

Kiernan, D., Hawkins, D.A., Christiansen, B.A., 2025. Differences in 10–20 Hz 'shock' attenuation emerge between injured and uninjured runners across a 30-minute run. J. Biomech. 196, 112955. https://doi.org/10.1016/j.jbiomech.2025.112955.

Luo, J., Ahmadvand, N., Crooks, M., 2025. Assessing loading rate in frequency domain by accelerometry. Proc. Inst. Mech. Eng. [H] 239 (11–12), 1147–1155. https://doi.org/10.1177/09544119251393825.

Malisoux, L., Gette, P., Backes, A., Herber-Losier, K., Urhausen, A., Theisen, D., 2021. Relevance of frequency-domain analyses to relate shoe cushioning, ground impact forces and running injury risk: a secondary analysis of a randomized trial with 800+ recreational runners. Front. Sports Active Living 3, 744658. https://doi.org/10.3389/fspor.2021.744658.

Pillitteri, G., Petrigna, L., Ficarra, S., Giustino, V., Thomas, E., Rossi, A., Clemente, F.M., Paoli, A., Petrucci, M., Bellafiore, M., Palma, A., Battaglia, G., 2024. Relationship between external and internal load indicators and injury using machine learning in professional soccer: a systematic review and meta-analysis. Res. Sports Med. 32 (6), 902–938. https://doi.org/10.1080/15438627.2023.2297190.

Radin, E.L., Yang, K.H., Riegger, C., Kish, V.L., O'Connor, J.J., 1991. Relationship between lower limb dynamics and knee joint pain. J. Orthop. Res. 9 (3), 398–405. https://doi.org/10.1002/jor.1100090312.

Rubin, C.T., Lanyon, L.E., 1984. Regulation of bone formation by applied dynamic loads. J. Bone Joint Surgery: American 66 (3), 397–402.

Schmitt, L.C., Paterno, M.V., Hewett, T.E., 2012. The impact of quadriceps femoris strength asymmetry on functional performance at return to sport following anterior cruciate ligament reconstruction. J. Orthop. Sports Phys. Ther. 42 (9), 750–759. https://doi.org/10.2519/jospt.2012.4194.

Shorten, M.R., Winslow, D.S., 1992. Spectral analysis of impact shock during running. Int. J. Sport Biomechanics 8 (4), 288–304. https://doi.org/10.1123/ijsb.8.4.288.

Vainionpää, A., Korpelainen, R., Vihriälä, E., Rinta-Paavola, A., Leppäluoto, J., Jämsä, T., 2006. Intensity of exercise is associated with bone density change in premenopausal women. Osteoporos. Int. 17 (3), 455–463. https://doi.org/10.1007/s00198-005-0005-x.

van Melick, N., Meddeler, B.M., Hoogeboom, T.J., Nijhuis-van der Sanden, M.W.G., van Cingel, R.E.H., 2017. How to determine leg dominance: the agreement between self-reported and observed performance in healthy adults. PLoS One 12 (12), e0189876. https://doi.org/10.1371/journal.pone.0189876.

Visuallex Sport International (n.d.) The VX System. https://www.vxsport.com/the-vx-system/. Accessed 13 May 2026.

Warden, S.J., Turner, C.H., 2004. Mechanotransduction in the cortical bone is most efficient at loading frequencies of 5–10 Hz. Bone 34 (2), 261–270. https://doi.org/10.1016/j.bone.2003.11.011.

Wylde, M.J., Callaway, A.J., Williams, J.M., Yap, J., Leow, S., Low, C.Y., 2022. Limb specific training magnitude and asymmetry measurement to discriminate between athletes with and without unilateral or bilateral lower limb injury history. Phys. Ther. Sport 56, 76–83. https://doi.org/10.1016/j.ptsp.2022.05.008.

Xiang, L., Gu, Y., Rong, M., Yang, T., Wang, A., Shim, V., Fernandez, J., 2022. Shock acceleration and attenuation during running with minimalist and maximalist shoes: a time- and frequency-domain analysis of tibial acceleration. Bioengineering 9 (7), 322. https://doi.org/10.3390/bioengineering9070322.